A Structural and Functional Model of Dinuclear Metallophosphatases

Nicholas H. Williams,*,† Anne-Marie Lebuis,‡ and Jik Chin*,‡

Contribution from the Departments of Chemistry, Sheffield University, Sheffield, U.K. S3 7HF, and McGill University, Montréal, Canada H3A 2K6

Received August 4, 1998

Abstract: Hydrolysis of four substituted phenyl phosphate monoesters, each coordinated to a dinuclear Co(III) complex, was studied ($[Co_2(tacn)_2(OH)_2\{O_3P(OAr)\}]^{2+}$; tacn = 1,4,7-triazacyclononane; substituent *m*-F, *p*-NO_2 (**5a**); *p*-NO_2 (**5b**); *m*-NO_2 (**5c**); unsubstituted (**5d**)). Crystallographic data reveal that **5b** is an excellent structural model of the active sites of several phosphatases: protein phosphatase-1, kidney bean purple acid phosphatase, and calcineurin-α. All of these structures consist of two octahedral metal complexes connected by two oxygen bridges, forming a four-membered-ring diamond core. The pH−rate profile and the ^{18}O labeling experiment for the hydrolysis of **5b** indicates that the oxide bridging the two metal centers in the diamond core is acting as an intramolecular nucleophile for cleaving the coordinated phosphate monoester. The phosphate monoesters in this model system are hydrolyzed more rapidly than those in previously reported model systems. Hence, the dinuclear cobalt complexes **5** appear to be excellent structural and functional models of the above-mentioned phosphatases. The rate of hydrolysis of **5** is highly sensitive to the basicity of the leaving group (β_{lg} = −1.10). Detailed analysis of the leaving group dependence for the hydrolysis of **5** indicates only a partial negative charge on the leaving group oxygen at the transition state, further supporting the nucleophilic mechanism.

Introduction

Recently, the structures of several dinuclear metallophosphatases [kidney bean purple acid phosphatase (KBPAP),[1] protein phosphatase-1 (PP-1),[2] and calcineurin α (PP-2B)][3] were reported. Although the amino acid sequences of the three enzymes are unrelated, the active site structures are strikingly similar. These enzymes all catalyze the hydrolysis of phosphate monoesters and have a "dimetallic diamond core". The active site of KBPAP contains a dinuclear Zn(II)−Fe(III) center with an intermetal distance of 3.1 Å. The two metal ions are both held in octahedral coordination geometries and are connected by two oxygen bridges (**1**), forming the four-membered-ring diamond core. Inorganic phosphate, the product of the hydrolysis reaction, was shown to bridge the two metal centers in the enzyme (**2**).[4] The active site structure of PP-1, with a tungstate inhibitor bound, also shows two metal ions [Mn(II) and Fe(II)] held in very similar coordination spheres (**3**), with the tungstate bridging the two metal ion centers. This enzyme acts on phosphorylated serine and threonine side chains, thereby playing an important role in signal transduction.[5] PP-2B has a similar role, and at its active site it has a very similar ligand grouping around Zn(II) and Fe(III) ions (**4**).

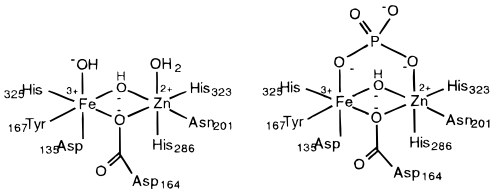

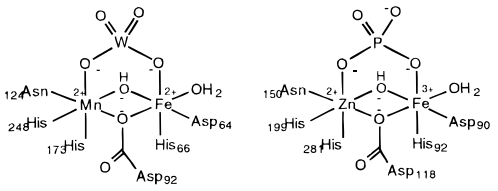

We have reported on the reactivity of phosphate diesters coordinated to a simple dinuclear Co(III) complex whose structure closely resembles those of the above-mentioned phosphatase active sites.[6] Here we report on the reactivity and structure of phosphate monoesters coordinated to the dinuclear Co(III) complex (**5**). The product of this reaction has inorganic phosphate bridging the two metal centers in the diamond core (**6**), much like in **2**, **3**, and **4**. It is of considerable interest to study the hydrolysis of phosphate monoesters separately from the hydrolysis of the diesters, not only because the monoesters are true substrates of the above phosphatases but also because the mechanisms of solvent-catalyzed hydrolysis of the diesters

† Sheffield University.

‡ McGill University.

(1) Sträter, N.; Klabunde, T.; Tucker, P.; Witzel, H.; Krebs, B. *Science* **1995**, *268*, 1489.

(2) (a) Goldberg, J.; Huang, H.-B.; Kwon, Y.-G.; Greenbard, P.; Nairn, A. C.; Kuriyan, J. *Nature* **1995**, *376*, 745. (b) Egloff, M.-P.; Cohen, P. T. W.; Reinemer, P.; Barford, D. *J. Mol. Biol.* **1995**, *254*, 942.

(3) (a) Griffith, J. P.; Kim, J. L.; Kim, E. E.; Sintchak, M. D.; Thomson, J. A.; Fitzgibbon, M. J.; Fleming, M. A.; Caron, P. R.; Hsaio, K.; Navia, M. A. *Cell* **1995**, *82*, 507. (b) Kissinger, C. R.; Parge, H. E.; Knighton, D. R.; Lewis, C. T.; Pelletier, L. A.; Tempczyk, A.; Kalish, V. J.; Tucker, K. D.; Showalter, R. E.; Moomaw, E. W.; Gastinel, L. N.; Habucka, N.; Chen, X.; Maldonado, F.; Barker, J. E.; Bacquet, R.; Villafranca, E. *Nature* **1995**, *378*, 641.

(4) Klabunde, T.; Sträter, N.; Frohlich, R.; Witzel, H.; Krebs, B. *J. Mol. Biol.* **1996**, *259*, 737.

(5) (a) Barford, D. *Trends Biochem. Sci.* **1996**, *21*, 407 and references therein. (b) Widlanski, T. S.; Myers, J. K.; Stec, B.; Holtz, K. M.; Kantowitz, E. R. *Chem. Biol.* **1997**, *4*, 489 and references therein.

(6) (a) Wahnon, D.; Lebuis, A.-M.; Chin, J. *Angew. Chem., Int. Ed. Engl.* **1995**, *34*, 2412. (b) Williams, N. H.; Chin, J. *J. Chem. Soc., Chem. Commun.* **1996**, 131. (c) Williams, N. H.; Cheung, W.; Chin, J. *J. Am. Chem. Soc.* **1998**, *120*, 8079.

10.1021/ja9827797 CCC: $18.00
Published on Web 03/23/1999

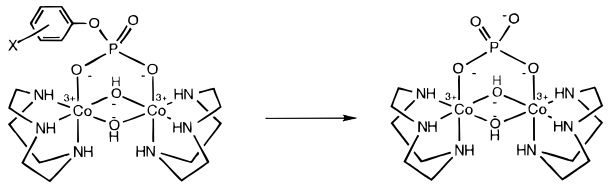

5a X = 3-F, 4-NO_2
5b X = 4-NO_2
5c X = 3-NO_2
5d X = H

6

and the monoesters are usually different. In the absence of any added catalysts, the monoesters generally hydrolyze by a dissociative mechanism,[7] while the diesters generally hydrolyze by a nucleophilic mechanism.

Experimental Section

Instruments. ^{1}H NMR (200 MHz) and ^{13}C NMR (50.3 MHz) spectra were obtained with a Gemini 200 spectrometer, while ^{31}P NMR spectra were obtained with a Varian XL-300 FT spectrometer (121.4 MHz) or a Varian Unity 500 FT spectrometer (202.5 MHz). Chemical shifts are reported in ppm with 3-(trimethylsilyl)-1-propane sulfonic acid (0 ppm), trimethyl phosphate (0 ppm), and dioxane (67.4 ppm) used as references for ^{1}H, ^{31}P, and ^{13}C NMR, respectively.

Kinetic studies were carried out by monitoring UV−vis changes with a Hewlett-Packard 8452A diode array spectrometer, equipped with a Lauda RM6 thermostat, or a Cary 1 Bio spectrometer. Product analyses by HPLC were performed on a Hewlett-Packard 1090 series II liquid Chromatograph using a 2.1-mm × 100-mm Hypersil ODS C-188 reversed-phase column.

Materials. The perchlorate salts of **5a**−**d** were synthesized following the same general procedure for making the perchlorate salt of the dinuclear complex with bridging diesters and showed the characteristic ∼14-ppm downfield shift relative to the unbound monoester in the ^{31}P NMR. Shifts are quoted downfield relative to an external trimethyl phosphate standard (10% trimethyl phosphate in D_2O).

General Procedure for Synthesis of 5a−**d.** [(1,4,7-Triazacyclononane)$_2$Co$_2$(OH)$_3$](ClO$_4$)$_3$ (25 mg, 34 μmol) is mixed with 1 mol equiv of phosphate monoester and 0.5 cm^3 of 1.0 M perchloric acid. The mixture is warmed gently to give a clear red-purple solution and allowed to cool slowly. If crystals could not be isolated after 12 h at 4 °C, the product complex was precipitated by adding solid sodium perchlorate and recrystallized from 0.01 M perchloric acid (yields ranged from 50 to 60%).

Complex 5a: δ_H (D_2O, 0.01 M $HClO_4$) 2.40−2.70 (12H, m, CH_2N), 3.00−3.30 (12H, m, CH_2N), 6.13 (2H, bs, NH), 6.17 (2H, bs, NH), 6.52 (2H, bs, NH), 7.00−7.11 (2H, m, ArH), 8.08 (1H, dd, J = 10.4 and 9.0 Hz); δ_P (D_2O, 0.01 M $HClO_4$) 8.45.

Anal. Calcd for $C_{18}H_{35}Cl_2Co_2FN_7O_{16}P\cdot H_2O$: C, 25.07; H, 4.33; N, 11.37; Co, 13.67. Found: C, 25.24; H, 4.33; N, 11.25; Co, 13.88.

Complex 5b: δ_H (D_2O, 0.01 M $HClO_4$) 2.40−2.70 (12H, m, CH_2N), 3.00−3.30 (12H, m, CH_2N), 6.10 (2H, bs, NH), 6.19 (2H, bs, NH), 6.53 (2H, bs, NH), 7.26 (2H, d, J = 9.2 Hz, ArH), 8.17 (2H, d, J = 9.2 Hz, ArH); δ_H (D_2O, 0.01 M $HClO_4$) 9.63.

Anal. Calcd for $C_{18}H_{36}Cl_2Co_2N_7O_{16}P\cdot H_2O$: C, 25.61; H, 4.54; N, 11.61; Co, 13.96. Found: C, 25.40; H, 4.51; N, 11.33; Co, 14.05.

Complex 5c: δ_H (CD_3CN) −1.20 (1H, s, μOH), −0.88 (1H, s, μOH), 1.80−2.10 (12H, m, CH_2N), 2.20−2.60 (12H, m, CH_2N), 5.68 (2H, bs, NH), 6.09 (4H, bs, NH), 7.03−7.13 (2H, m, ArH), 7.38−7.46 (1H, m, ArH), 7.55 (1H, s, ArH); δ_H (D_2O) 9.65.

Complex 5d: δ_H (DMSO) −0.66 (1H, s, μOH), −0.38 (1H, s, μOH), 2.35−2.75 (12H, m), 2.85−3.20 (12H, m), 6.31 (2H, bs, NH), 6.71 (4H, bs, NH), 7.12 (1H, t, J 7.6 Hz), 7.23 (2H, d, J = 7.6 Hz), 7.35 (2H, t, J = 7.6 Hz); δ_H (D_2O, 0.01 M $HClO_4$) 9.63.

Anal. Calcd for $C_{18}H_{37}Cl_2Co_2N_6O_{14}P\cdot HClO_4$: C, 24.52; H, 4.34; N, 9.53; Co, 13.37. Found: C, 24.78; H, 4.54; N, 9.39; Co, 13.32.

Product Analysis. ^{31}P NMR reveals that **5a**−**c** (10 mM, 8.74 ppm) react in a buffered solution (100 mM CHES, 1:1 H_2O/D_2O by volume) at pH 10.0, 25 °C, to give **6** (15.05 ppm). Complex **6** was identified by ^{31}P NMR as follows. Inorganic phosphate was used to replace phosphate monoester in the synthesis, and the reaction mixture showed a single peak in the ^{31}P NMR spectrum at 15 ppm after reaching equilibrium. This solution was mixed with the sample of hydrolyzed **5a**−**c**, giving a single peak at 15.05 ppm. Released phenol was identified by HPLC comparison with authentic samples. **5d** reacted to give phenol and **6** and also phenyl phosphate (identified through HPLC and ^{31}P NMR); the percentage hydrolysis is 55%, as measured by integrating the ^{31}P NMR signals and by normalizing the HPLC trace of the product mixture with authentic samples.

The pK_as of the leaving group phenols were determined by titration under our experimental conditions [I = 0.1 M ($NaClO_4$), titrant 0.1 M NaOH] and gave values of 6.10 for 3-F,4-NO_2 phenol, 6.95 for 4-NO_2 phenol, 7.95 for 3-NO_2 phenol, and 9.90 for phenol. These values are used in this paper where our data are reported.

Kinetic Methods. Hydrolysis of the complexes [0.05 mM in 50 mM aqueous buffer, I = 0.1 M ($NaClO_4$), at 25 °C] was followed by monitoring the increase in absorbance at 400 nm for **5a**−**c** (**5d** was monitored at 300 nm) and accurately obeyed first-order kinetics for at least 5 half-lives. At pH > 10, **5b** was monitored by using a stopped-flow spectrometer, for which we are grateful to Prof. R. S. Brown, Queen's University, Kingston, ON, Canada. The observed rate constants for **5d** were corrected for the proportion of dissociation measured in the product analysis to give the observed rate constants for hydrolysis.

As doubling the buffer concentration did not increase the observed rate constants within experimental error, extrapolation to zero buffer was not necessary. pHs were measured before and after each reaction, and did not change. Buffers used were 2-(*N*-morpholino)ethanesulfonic acid (MES), *N*-(2-hydroxyethyl)piperazine-*N*′-(2-ethanesulfonic acid) (HEPES), *N*-(2-hydroxyethyl)piperazine-*N*′-(2-propanesulfonic acid) (EPPS), 2-(*N*-cyclohexylamino)ethanesulfonic acid (CHES), 3-(*N*-cyclohexylamino)-1-propanesulfonic acid (CAPS), and NaOH above pH 12.

Isotopic Labeling Studies. Complex **5b** was hydrolyzed in buffered, aqueous solution at pH 9.0 which was 50% labeled with $^{18}OH_2$ and analyzed by ^{31}P NMR at 202 MHz. **5b** was also synthesized with the bridging hydroxides 50% labeled with ^{18}O by using 50% $^{18}OH_2$ as solvent for the synthesis of the triol and for the complexation steps. This labeled species was then hydrolyzed in $^{16}OH_2$ buffered, aqueous solution and analyzed as above.

Solvent Isotope Effect. The deuterium solvent isotope effect for **5b** was determined at 25 °C in CHES and EPPS buffers, made up as described above but with >98% D_2O as solvent. The reaction was measured at pDs 8.58, 8.95, and 9.94, where pD = pH meter reading + 0.40, and gave a pD−rate profile of slope 1.

Activation Parameters. The Arrhenius parameters for **5b** were obtained by measuring the observed rate constants at 25, 30, 40, 50, and 60 °C at pHs ∼7.7, ∼8.2, ∼8.6, and ∼9.0 in each case (determined by measuring the pH of each reaction mixture under the experimental conditions; the same buffer mixtures were used for each temperature). The value of k_h was calculated from each of these profiles (which gave pH−rate profiles of slope 1 in each case) using the appropriate value of K_w. These data were plotted as $\ln(k_h)$ against $1/T$ and fitted to $\ln(k_h) = \ln A + E_a/(RT)$. Linear least-squares regression gave the Arrhenius parameters E_a = 56 ± 2 kJ mol^{-1}and $\ln A$ = 28.6 ± 0.6. These were converted to the activation parameters at 25 °C by applying the equations $\Delta H^{\ddagger} = E_a - RT$ and $\Delta S^{\ddagger} = R \ln A - R \ln(k\ \mathrm{Te}/\hbar) = R \ln A - 253.24$ J mol^{-1} K^{-1} (at 25 °C; k is the Boltzmann constant and $\hbar$ is the Planck constant).

X-ray Diffraction Study of 5b·HClO$_4$·2H$_2$O·2ClO$_4$. The intensity data were collected using graphite-monochromatized Mo Kα radiation (0.710 69 Å) on a Rigaku AFC6S diffractometer. The $\omega-2\theta$ scan mode

(7) It should be noted that a fully dissociative mechanism involves the formation of a meta-phosphate intermediate with complete bond cleavage (to the leaving group) before any bond formation (to the nucleophile). A fully associative mechanism involves complete bond formation (to the nucleophile) before any bond cleavage (to the leaving group). A concerted mechanism could be said to be associative or dissociative, depending on the extent of bond formation and cleavage at the transition state. Thus, concerted mechanisms involving substantial bond cleavage with little bond formation at the transition state are also referred to as dissociative.

Table 1. Crystallographic Data for **5b**·$HClO_4$·$2H_2O$·$2ClO_4$

molecular formula	$C_{18}H_{41}O_{22}N_7PCl_3Co_2$
molecular weight	962.75
crystal system	monoclinic
space group	$P2_1/c$
a (Å)	18.554(4)
b (Å)	10.388(8)
c (Å)	19.505(5)
β (deg)	107.23(1)
V (Å^3)	3591(3)
Z	4
ρ_{calc} (g cm^{-3})	1.781
crystal dimensions (mm)	0.46 × 0.23 × 0.11
temperature (°C)	20 ± 1
μ (mm^{-1})	1.282
h, k, l limits	−22 to 22, 0 to 12, −23 to 23
$2\theta_{max}$ (deg)	50.0
F(000)	1976
no. of data collected	10 803
no. of unique data	5449
no. of data with $I > 2.0\sigma(I)$	2453
no. of variables	407
R^a	0.061
$R_w{}^b$	0.064
R_{int}	0.116
goodness of fit^c	1.65
last ΔF (e Å^{-3})	0.56 to −0.56

Table 2. Selected Distances (Å) and Angles (deg) for **5b**·$HClO_4$·$2H_2O$·$2ClO_4$

Bond Distances			
Co(1)−O(1)	1.920(8)	Co(2)−O(1)	1.930(7)
Co(1)−O(2)	1.908(7)	Co(2)−O(2)	1.919(8)
Co(1)−O(3)	1.934(7)	Co(2)−O(4)	1.929(8)
Co(1)−N(1)	1.915(9)	Co(2)−N(4)	1.90(1)
Co(1)−N(2)	1.94(1)	Co(2)−N(5)	1.93(1)
Co(1)−N(3)	1.95(1)	Co(2)−N(6)	1.94(1)
Nonbonding Distances			
Co(1)···Co(2)	2.910(3)	O(1)···P(1)	3.075(8)
O(1)···O(2)	2.43(1)	O(2)···P(1)	3.294(8)
Bond Angles			
O(1)−Co(1)−O(2)	78.8(3)	O(1)−Co(2)−O(2)	78.3(3)
O(1)−Co(1)−O(3)	94.8(3)	O(1)−Co(2)−O(4)	96.5(3)
O(1)−Co(1)−N(1)	90.7(4)	O(1)−Co(2)−N(4)	90.9(4)
O(1)−Co(1)−N(2)	173.3(4)	O(1)−Co(2)−N(5)	174.4(4)
O(1)−Co(1)−N(3)	99.0(4)	O(1)−Co(2)−N(6)	98.2(4)
O(2)−Co(1)−O(3)	95.8(3)	O(2)−Co(2)−O(4)	92.3(3)
O(2)−Co(1)−N(1)	90.4(3)	O(2)−Co(2)−N(4)	92.4(3)
O(2)−Co(1)−N(2)	95.2(4)	O(2)−Co(2)−N(5)	97.2(4)
O(2)−Co(1)−N(3)	176.2(4)	O(2)−Co(2)−N(6)	176.0(3)
O(3)−Co(1)−N(1)	172.4(4)	O(4)−Co(2)−N(4)	171.9(4)
O(3)−Co(1)−N(2)	88.5(4)	O(4)−Co(2)−N(5)	87.0(4)
O(3)−Co(1)−N(3)	87.4(4)	O(4)−Co(2)−N(6)	90.1(4)
N(1)−Co(1)−N(2)	86.5(4)	N(4)−Co(2)−N(5)	85.9(4)
N(1)−Co(1)−N(3)	86.6(4)	N(4)−Co(2)−N(6)	85.6(4)
N(2)−Co(1)−N(3)	86.9(4)	N(5)−Co(2)−N(6)	86.1(4)
Co(1)−O(1)−Co(2)	98.2(3)	Co(1)−O(2)−Co(2)	99.9(4)

was used. All calculations were performed using the TEXSAN crystallographic software package.[8] The structure was solved by direct methods followed by a difference Fourier analysis. Data are summarized in Table 1 and Figure 5. Seclected distances and angles are listed in Table 2, while positional parameters are given in Table 3.

Complex **5b** was recrystallized from 0.01 M $HClO_4$, yielding a red, narrow crystal (**5b**·$HClO_4$·$2H_2O$·$2ClO_4$, formula weight 962.75), which was mounted on a glass fiber. Lattice parameters for **5b** were determined by least-squares refinement using the setting angles of 20 carefully centered reflections in the range $20.00 < 2\theta < 30.00°$. Data were collected to a maximum 2θ of 50°. The cell is monoclinic, space group $P2_1/c$, with dimensions $a = 18.554(4)$ Å, $b = 10.388(8)$ Å, $c = 19.505(5)$ Å, $\beta = 107.23(1)°$, and $V = 3591(3)$ Å^3, with $Z = 4$. Hydrogen atoms were introduced at idealized geometries; hydrogens on OH groups and one water molecule [O((W)2)] were located in a difference map. H atoms on the other water molecule were not included in the model. All three perchlorates showed important thermal motion, but only one (ClO_4 no. 2)) clearly showed disorder. This was refined with two orientations for the oxygen atoms at occupancies 0.67 and 0.33. Non-hydrogen atoms were refined anisotropically, except for the nitrophenyl group and oxygens from the minor orientation of ClO_4 no. 2. The data were corrected for Lorentz and polarization effects. The final cycle of full-matrix least-squares refinement was based on 2453 observed reflections ($I > 2.00\sigma(I)$) and 407 variable parameters and converged with agreement factors of $R = 0.061$ and $R_w = 0.064$ (goodness of fit

Table 3. Positional Parameters for **5b**·$HClO_4$·$2H_2O$·$2ClO_4$

atom	x	y	z	B(eq)
Co(1)	0.29493(09)	0.26108(16)	0.34833(08)	2.27(6)
Co(2)	0.24184(09)	0.46348(16)	0.24222(08)	2.42(7)
P(1)	0.2334(02)	0.1877(03)	0.19189(17)	3.0(1)
O(1)	0.3354(04)	0.3822(07)	0.2950(03)	2.8(3)
O(2)	0.2140(04)	0.3816(07)	0.3189(04)	2.5(3)
O(3)	0.2567(04)	0.1444(07)	0.2686(04)	3.1(4)
O(4)	0.2037(04)	0.3219(07)	0.1777(04)	3.3(4)
O(5)	0.1701(05)	0.0863(08)	0.1543(04)	4.1(4)
O(6)	0.2970(05)	0.1757(09)	0.1564(05)	4.7(4)
O(7)	−0.0480(06)	0.1217(10)	−0.1567(05)	6.1(2)
O(8)	0.0182(06)	−0.0395(11)	−0.1691(05)	6.2(3)
N(1)	0.3375(05)	0.3566(09)	0.4349(04)	2.6(4)
N(2)	0.2469(05)	0.1551(09)	0.4040(05)	2.7(4)
N(3)	0.3819(05)	0.1475(09)	0.3810(05)	2.9(4)
N(4)	0.2704(06)	0.6179(10)	0.2956(05)	3.2(5)
N(5)	0.1468(05)	0.5482(10)	0.1984(05)	3.2(5)
N(6)	0.2771(05)	0.5473(09)	0.1693(05)	3.2(5)
N(7)	0.0037(06)	0.0491(11)	−0.1360(06)	4.2(2)
C(1)	0.3047(08)	0.3143(13)	0.4921(08)	4.3(7)
C(2)	0.2368(08)	0.2410(15)	0.4603(07)	4.4(7)
C(3)	0.2937(07)	0.0389(14)	0.4307(07)	4.5(7)
C(4)	0.3520(08)	0.0223(13)	0.3960(07)	4.3(7)
C(5)	0.4380(08)	0.2036(16)	0.4450(08)	5.4(8)
C(6)	0.4214(08)	0.3374(15)	0.4543(07)	4.9(7)
C(7)	0.2082(09)	0.7083(15)	0.2873(08)	6.0(8)
C(8)	0.1379(08)	0.6422(16)	0.2517(08)	5.4(8)
C(9)	0.1458(08)	0.6060(16)	0.1294(07)	5.1(7)
C(10)	0.2091(08)	0.5668(16)	0.1056(07)	5.3(7)
C(11)	0.3194(08)	0.6645(14)	0.1964(07)	5.0(7)
C(12)	0.3323(09)	0.6735(14)	0.2723(08)	5.6(8)
C(13)	0.1327(07)	0.0851(12)	0.0799(06)	3.2(3)
C(14)	0.0795(07)	0.1785(13)	0.0512(07)	4.0(3)
C(15)	0.0388(07)	0.1675(13)	−0.0212(07)	3.8(3)
C(16)	0.0519(06)	0.0658(11)	−0.0590(06)	2.9(2)
C(17)	0.1068(07)	−0.0268(12)	−0.0310(06)	3.3(3)
C(18)	0.1480(06)	−0.0149(11)	0.0424(06)	2.8(2)
Cl(1)	0.3519(02)	−0.3147(04)	0.5036(02)	4.4(2)
O(9)	0.3980(07)	−0.3996(10)	0.5519(06)	8.0(6)
O(10)	0.3801(08)	−0.3026(15)	0.4456(06)	11(1)
O(11)	0.3524(08)	−0.1942(11)	0.5324(06)	9.8(7)
O(12)	0.2830(08)	−0.3641(14)	0.4780(11)	16(1)
Cl(2)	0.0707(02)	−0.0619(04)	0.3920(02)	5.2(2)
O(13)	0.1141(09)	−0.0320(19)	0.3398(08)	8.0(5)
O(14)	−0.0024(07)	−0.083(02)	0.3579(11)	11(1)
O(15)	0.0814(12)	0.0585(17)	0.4370(11)	12.7(8)
O(16)	0.1102(11)	−0.1620(16)	0.4373(10)	10.8(6)
O(13)	0.075(02)	0.057(02)	0.370(02)	13(1)
O(14)	0.065(02)	−0.078(04)	0.4638(11)	13(1)
O(15)	0.1297(14)	−0.149(03)	0.384(02)	13(1)
O(16)	−0.0023(13)	−0.126(03)	0.3442(02)	6(1)
Cl(3)	0.4659(02)	0.3752(06)	0.1679(02)	6.2(2)
O(17)	0.3958(06)	0.4165(11)	0.1223(06)	7.2(6)
O(18)	0.4573(06)	0.3375(15)	0.2348(06)	10.3(8)
O(19)	0.4893(09)	0.269(02)	0.1391(08)	16(1)
O(20)	0.5229(08)	0.466(10)	0.1801(07)	16(1)
O((W)1)	0.6239(06)	0.0303(10)	0.8185(05)	6.6(3)
O((W)2)	0.0778(06)	0.2475(10)	0.2769(05)	6.6(3)

(8) *TEXSAN Structure Analysis Package*; Molecular Structure Corp.: The Woodlands, TX, 1985.

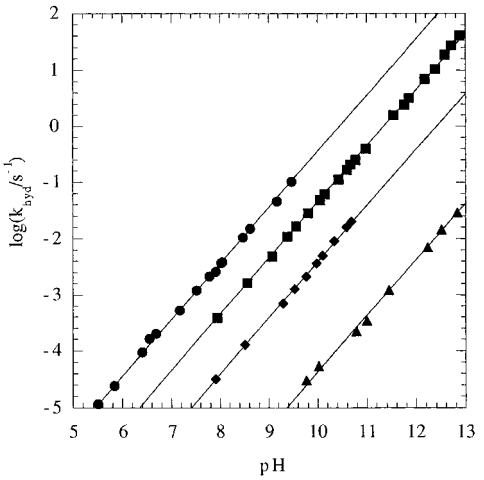

Figure 1. pH−rate profiles for the hydrolysis of **5a** (●), **5b** (■), **5c** (◆), and **5d** (▲). Linear least-squares regression was used to fit these data to a slope of 1 (solid lines).

Scheme 1. Proposed Mechanism of Hydrolysis of **5**

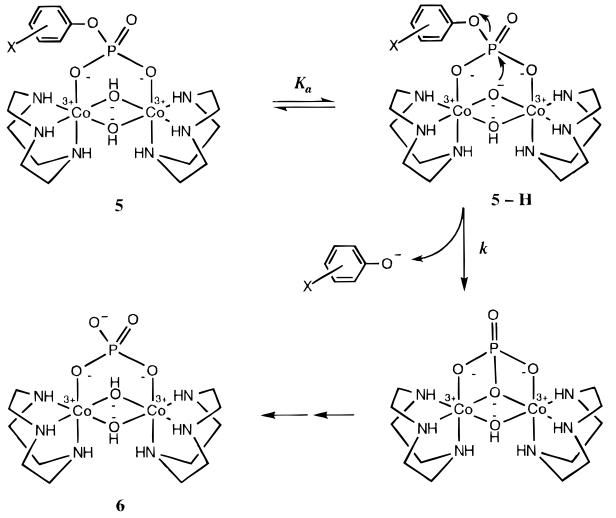

= 1.65). The high agreement factors reflect thermal motion in the perchlorate groups.

Results and Discussion

Mechanism and Reactivity. In all cases except for that of **5d**, the coordinated phosphates in **5** are cleanly hydrolyzed to **6** and the corresponding phenol only. Dissociation of phenyl phosphate from **5d** competes with hydrolysis but is irreversible at the pHs monitored, as the dinuclear complex rearranges to the triply hydroxide-bridged complex.[9] The percentage of dissociation for **5d** is approximately 45%. At all pHs studied, we find that the first-order rate constants for hydrolysis fit eq 1 accurately (Figure 1), giving values of $k_h = 3540 \pm 90$ (**5a**), 449 ± 7 (**5b**), 38.3 ± 0.6 (**5c**), and 0.23 ± 0.01 M^{-1} s^{-1} (**5d**).

$$k_{obs} = k_h[HO^-] \quad (1)$$

Similarly to related dinuclear complexes containing phosphate diesters,[6a,c] we propose a mechanism in which a bridging oxide (**5-H**, Scheme 1) attacks the phosphate, displacing the phenolate and subsequently rearranging to form **6**. To examine this hypothesis, we labeled the solvent with $^{18}OH_2$ (50 vol %). If

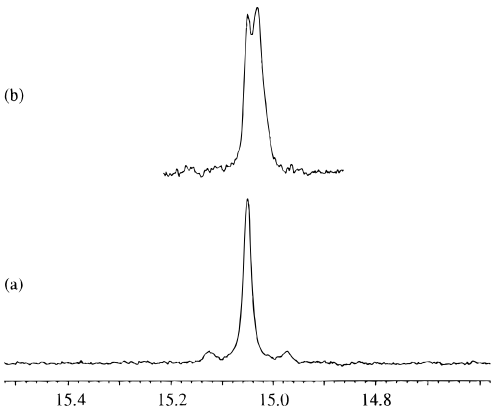

Figure 2. ^{31}P NMR spectra of **6** from hydrolysis of **5b** with (a) solvent 50% labeled with ^{18}O and (b) bridging hydroxides 50% labeled with ^{18}O.

the incoming oxygen nucleophile comes from the solvent (either directly or via coordination with a Co(III) center), then the product ^{31}P NMR signal would be split into two signals due to the ∼0.02 ppm shift brought about by ^{18}O incorporation into 50% of the product.[10] No splitting is observed (Figure 2a). However, by labeling the bridging hydroxides with 50% ^{18}OH and conducting the analysis in unlabeled solvent, we find that ^{18}O is incorporated into the product, shown by the appearance of an apparent doublet with a separation of ∼0.02 ppm (Figure 2b). Presumably, the two bridging hydroxides in **5b** do not exchange with solvent, as they are doubly coordinated to the substitutionally inert Co(III) centers.

Consistent with our mechanism is an inverse solvent isotope effect of 0.56 on the second-order lyonium-catalyzed hydrolysis of **5b**, which is comparable to the measured isotope effect for the analogous bridging diester (0.55, ref 6c). Considering the mechanism in Scheme 1, $k_h = kK_a/K_w$. The solvent isotope effect on k is expected to be small (∼1.1), as is typical for nucleophilic attack, and the effect on K_a usually lies in the range 2.5−4 (or ΔpK_a of 0.4−0.6). Thus, as $K_w^{D_2O}/K_w^{H_2O}$ has a value of 0.135 at 25 °C,[11] an overall effect of 0.56 is explained by a solvent isotope effect of 3.8 on K_a (i.e., $0.135 \times 3.8 \times 1.1 = 0.56$).

The pH−rate profile for the hydrolysis of **5b** (Figure 1) shows no sign of deviation from linearity up to pH 13 (and up to pH 14 at higher ionic strength), indicating that the kinetic pK_a of the bridging hydroxide is greater than 14 under our conditions. We estimate the pK_a of the bridging hydroxide as 15 by comparison with the pK_a for deprotonation of hydroxide in a similar dinuclear Co(III) complex with three bridging hydroxides.[12] The pH−rate profile also shows no deviation from linearity down to pH 5.5 for **5a**, indicating that the bridging oxide is the only kinetically significant nucleophile down to at least pH 4.5 (i.e., the bridging hydroxides are not nucleophiles at any pH monitored here).

The activation parameters for the hydroxide-catalyzed hydrolysis of **5b** are $\Delta H^{\ddagger} = 53 \pm 2$ kJ mol^{-1} and $\Delta S^{\ddagger} = -16 \pm 5$ J mol^{-1} K^{-1}. By comparison, those for hydroxide-catalyzed hydrolysis of methyl 4-nitrophenyl phosphate bridging the dinuclear complex are $\Delta H^{\ddagger} = 47 \pm 2$ kJ mol^{-1} and $\Delta S^{\ddagger} = -0.7 \pm 7$ J mol^{-1} K^{-1}. Both the enthalpic and entropic barriers are higher for the monoester than for the diester, as might be expected for bringing a dianionic nucleophile (oxide) to a

(9) Wieghardt, K.; Schmidt, W.; Nuber, B.; Weiss, J. *Chem. Ber.* **1979**, *112*, 2220.

(10) Cohn, M.; Hu, A. *Proc. Natl. Acad. Sci. U.S.A.* **1978**, *75*, 200.

(11) (a) Marshall, W. L.; Franck, E. U. *J. Phys. Chem. Ref. Data* **1981**, *10*, 295. (b) Mesmer, R. E.; Herting, D. L. *J. Solution Chem.* **1978**, *7*, 901.

(12) Käler, H. C.; Geier, G.; Schwarzenbach, G. *Helv. Chim. Acta* **1974**, *57*, 802.

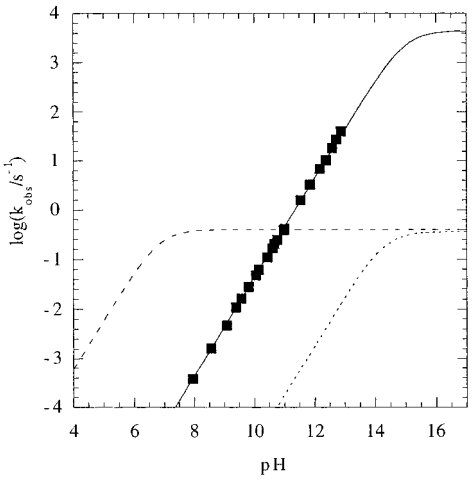

Figure 3. pH−rate profiles of **5b** (■), **7** (···) and **8** (- - -). The fits are constructed from the reported data, assuming that the ionized forms of **5b**, **7**, and **8** are the only reactive species, with pK_as of 15 (**5b** and **7**) and 7.5 (**8**).

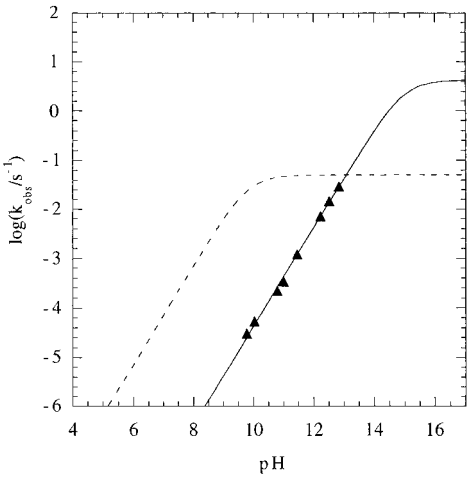

Figure 4. pH−rate profiles of **5d** (▲) and **9** (- - -). The fits are constructed from the reported data, assuming that the ionized forms of **5d** and **9** are the only reactive species, with pK_as of 15 (**5d**) and 9.85 (**9**).

dianionic electrophile (monoester) rather than to a monoanionic electrophile (diester).

The pseudo-first-order rate constant for the hydrolysis of 4-nitrophenyl phosphate in 0.5 M NaOH at 25 °C is about 2×10^{-9} s^{-1}.[13] Under the same conditions, the coordinated monoester in **5b** would have a pseudo-first-order rate constant of 200 s^{-1}, representing a 10^{11}-fold rate acceleration for phosphate monoester hydrolysis. However, detailed comparison of the rate difference between the two reactions is not very meaningful, as the background reaction follows a different mechanism and is pH-independent in this region. The background reaction is dissociative in character,[14] involving a meta-phosphate intermediate in contrast to the nucleophilic mechanism which is proposed here fphophateor the hydrolysis of the metal-coordinated phophate (Scheme 1). The observed requirement of an oxide nucleophile (pH−rate profile, ^{18}O labeling experiment) for the large rate accelerations strongly supports the nucleophilic mechanism (Scheme 1). Nucleophilic mechanisms have also been advanced for other simple metal ion complex and metalloenzyme-catalyzed hydrolysis of phosphate monoesters (see below).

We can compare the reactivity of 4-nitrophenyl phosphate in **5b** to that of the same monoester in other dinuclear Co(III) complexes, **7**[15] and **8**[16] (Figure 3). Sargeson et al.[15,16] showed

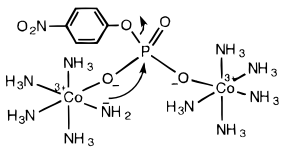

7

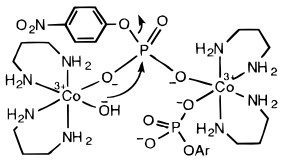

8

that hydrolysis of the phosphate in **7** and **8** competes with dissociation of the phosphate from the cobalt complexes as part of a complex series of events. The proposed mechanism for cleavage of 4-nitrophenyl phosphate in **7** or **8** involves deprotonation of one of the cobalt-coordinated ammonia (**7**) or water (**8**) molecules, followed by intramolecular nucleophilic attack of the anion on the phosphate. Comparing the systems, the pK_as of the conjugate acids of **5-H** and **7** are both expected to be approximately 15. As the second-order rate constant for hydroxide-catalyzed hydrolysis of the phosphate monoester in **7** is 0.034 M^{-1} s^{-1} at 25 °C, the monoester in **5b** is hydrolyzed (449 M^{-1} s^{-1}) about 4 orders of magnitude faster than that in **7** at all pHs (Figure 3). The rate of hydrolysis of the monoester in **8** is pH-independent above pH 8.5 (∼0.4 s^{-1}), as the nucleophile is in the hydroxide form under these conditions (pK_a ≤ 7.5). Hence, under neutral conditions, the monoester in **8** hydrolyzes more rapidly than that in **5b**. However, at pH ≥ 11, this is reversed. Comparing the rate of hydrolysis of **5-H** (∼4000 s^{-1}) with the value for **8** (in its fully ionized form) again gives a rate difference of about 4 orders of magnitude (Figure 3).

It is interesting to compare the reactivity of **5d** to that of another dinuclear cobalt complex with a bridging phenyl phosphate, **9**.[17] Complex **9** is a structural and functional model

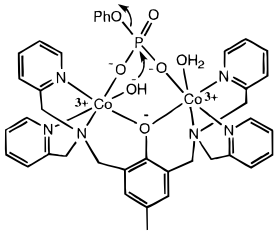

9

of D-fructose 1,6-biphosphate 1-phosphatase. Compared to **7** and **8** above, in **9** there are fewer rotational degrees of freedom between the bound phosphate and the metal-bound nucleophile. At neutral pH, phenyl phosphate in **9** hydrolyzes about 3 orders of magnitude more rapidly than that in **5d**. However, comparing the rate constants of the fully ionized species, **5d** is about 2 orders of magnitude more reactive than **9** (Figure 4).

Comparison with Enzymes. The similarities between the structure of **5b** (Figure 5) and those of the enzyme active sites (**2**, **3**, and **4**) are obvious. All of the structures consist of a dimetallic diamond core with two phosphoryl oxygens of a phosphate (or tungstate oxygens) bridging the two octahedral

(13) Extrapolated from data reported in the following: Kirby, A. J.; Jencks, W. P. *J. Am. Chem. Soc.* **1965**, *87*, 3209.

(14) Kirby, A. J.; Varvoglis, A. G. *J. Am. Chem. Soc.* **1967**, *89*, 415.

(15) Hendry, P.; Sargeson, A. M. *Inorg. Chem.* **1990**, *29*, 92.

(16) (a) Jones, D. R.; Lindoy, L. F.; Sargeson, A. M. *J. Am. Chem. Soc.* **1984**, *106*, 7807. (b) Anderson, B.; Milburn, R. M.; Harrowfield, J. MacB.; Robertson, G. B.; Sargeson, A. M. *J. Am. Chem. Soc.* **1977**, *99*, 2632.

(17) Seo, J. S.; Sung, N.-D.; Hynes, R. C.; Chin, J. *Inorg. Chem.* **1996**, *35*, 7472.

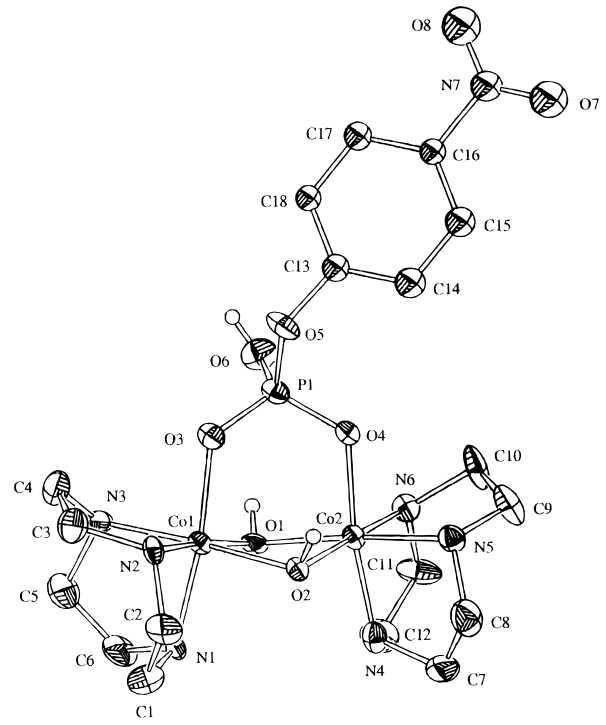

Figure 5. ORTEP plot of the cation of **5b**·$HClO_4$·$2H_2O$·$2ClO_4$. Thermal elipsoids are drawn at the 30% probability level.

Scheme 2. Proposed Mechanisms at the Active Site of KBPAP from (a) Ref 4 and (b) This Work

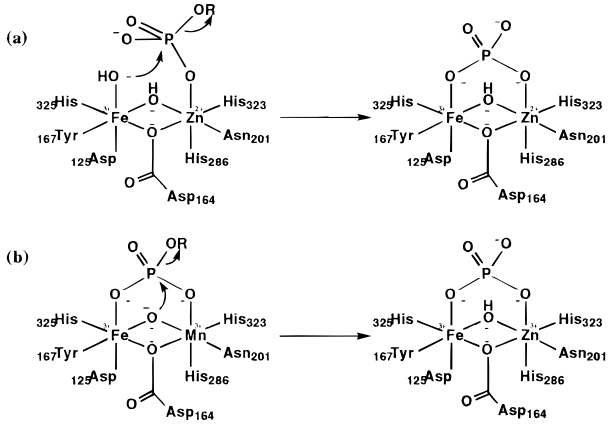

metal centers. The intermetal distance in **5b** (2.9 Å) is comparable to those reported for the enzymes (**2**, 3.1 Å;[1,4] **3**, 3.3,[2a] 3.3 Å[2b]; **4**, 3.0,[3a] 3.1 Å[3b]). The phosphorus center in **5b** is tilted to one side so that one of the bridging hydroxides is held very close to it (3.07 Å; the sum of the van der Waals radii of oxygen and phosphorus is 3.3 Å). Presumably, this close proximity with no rotational degress of freedom between the oxide and phosphorus leads to a highly efficient intramolecular reaction.

We suggest that phosphatases may also hydrolyze phosphate monoesters by a mechanism (Scheme 2b) that is analogous to the one proposed for our model system (Scheme 1). This mechanism contrasts with some previous proposals for KBPAP (Scheme 2a),[4] in which the monoester is singly coordinated with the zinc center and attacked by an iron-bound hydroxide. The two mechanisms give identical products and are kinetically indistinguishable. It is noteworthy that the pK_as of bridging hydroxides have been observed to be as low as 4 in dinuclear complexes made up of Fe(III) and Ru(III) in similar complexes,[18] and so it is possible that the natural systems may have considerably more acidic bridging hydroxides available than the model reported here. As discussed earlier, the reactivity of model systems **7** and **8**, which reflect Scheme 2a, is lower than the reactivity of the model system **5**, which reflects Scheme 2b.

The observation that PP-2B cannot catalyze the transesterification of esters[19] is perhaps better rationalized by the mechanism in Scheme 2b than the one in Scheme 2a, as alcohols cannot form oxide nucleophiles. In principle, the metal hydroxide mechanism (Scheme 2a) should also allow transesterification of phosphate monoesters by the corresponding metal alkoxide intermediate. Inversion at phosphorus has been demonstrated for the purple acid phosphatase-catalyzed reaction, implying that direct phosphate transfer to water is occurring.[20] This is consistent with both mechanisms in Scheme 2. In the reaction of **5b**, the incorporation of an oxygen atom from the bridge (Figure 2) implies that a single displacement step is occurring at the phosphorus center.

The crystal structure also shows that the leaving group can easily be positioned for an in-line displacement (μOH−P−OAr angle 165.2(4)°). Interestingly, in the crystal structure of PP-1 with tungstate inhibitor bound at the active site, the metal ion bridging hydroxide is poised in line with one of the W−O bonds and, on this basis, has been proposed as the active nucleophile. This "leaving group" O also hydrogen bonds with a histidine residue, and this is suggested as a possible general acid in the catalytic mechanism.[2b]

Transition-State Structure. It has been recently reported by Hollfelder and Herschlag[21] that alkaline phosphatase (AP)-catalyzed hydrolysis of thiophosphates is highly sensitive to the basicity of the leaving group ($\beta_{lg} = -0.77 \pm 0.09$), as is the solvent-catalyzed hydrolysis of the same substrates ($\beta_{lg} = -1.10 \pm 0.09$). Since the solvent-catalyzed reaction takes place by a dissociative mechanism,[13] these authors interpret their data as indicating a dissociative mechanism[7] for the enzyme-catalyzed reaction.[21] Thus, according to Hollfelder and Herschlag's interpretation, the enzyme has evolved to stabilize the solution transition state (i.e., dissociative) without significantly altering its structure; the reasoning implies that if the enzyme-catalyzed reaction follows a nucleophilic mechanism, the value of the β_{lg} would be small. Breslow and Katz came to the opposite conclusion, also based on experiments using a thiophosphate substrate.[22] They focused on the decreased reactivity of *O*-4-nitrophenyl thiophosphate compared to that of the 4-nitrophenyl phosphate in the enzyme-catalyzed reaction. A similar "thio effect" is observed with the solvent-catalyzed hydrolysis of phosphate triesters,[23] which is known to follow a nucleophilic mechanism;[24] in contrast, solvent-catalyzed hydrolysis of phosphate monoesters has an inverse "thio effect", whereby the thio substitution accelerates the reaction ~10-fold.[25] Thus, Breslow

(18) Hotzelmann, R.; Wieghardt, K.; Ensling, J.; Romstedt, H.; Gütlich, P.; Bill, E.; Flörke, U.; Haupt, H.-J. *J. Am. Chem. Soc.* **1992**, *114*, 9470.
(19) (a) Martin, B. L.; Graves, D. J. *Biochim. Biophys. Acta* **1994**, *1206*, 136. (b) Martin, B. L.; Graves, D. J. *J. Biol. Chem.* **1986**, *261*, 14545. (c) Martin, B.; Pallens, C. J.; Wangs, J. H.; Graves, D. J. *J. Biol. Chem.* **1985**, *260*, 14932.
(20) Mueller, E. G.; Crowder, M. W.; Averill, B. A.; Knowles, J. R. *J. Am. Chem. Soc.* **1993**, *115*, 2974.
(21) Hollfelder, F.; Herschlag, D. *Biochemistry* **1995**, *34*, 12255.
(22) Breslow, R.; Katz, I. *J. Am. Chem. Soc.* **1968**, *90*, 7376.
(23) (a) Ketelaar, J. A. A.; Gersmann, H. R.; Koopmans, K. *Recl. Trav. Chim. Phys-Bas* **1952**, *71*, 1253. (b) Fanni, T.; Taira, K.; Gorenstein, D. G.; Vaidyanathaswany, R.; Verkade, J. G. *J. Am. Chem. Soc.* **1986**, *108*, 6311.
(24) Khan, S. A.; Kirby, A. J. *J. Chem. Soc. (B)* **1967**, 1172.
(25) (a) Domanico, P.; Mizrahi, V.; Benkovic, S. J. In *Mechanisms of Enzymatic Reactions: Stereochemistry*; Frey, P. A., Ed.; Elsevier: Amsterdam, 1986; pp 127−138. (b) Reference 19.

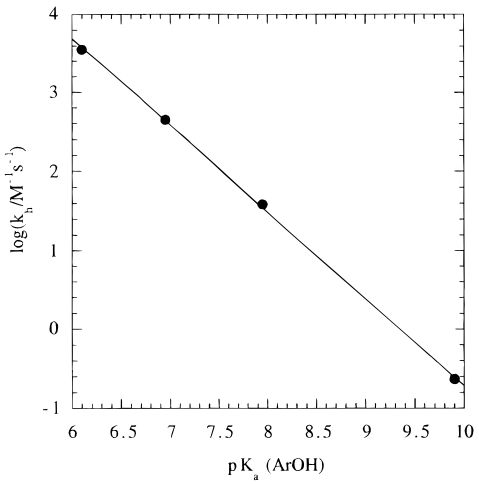

Figure 6. Linear free energy relationship between leaving group pK_a and second-order rate constant for hydroxide-catalyzed hydrolysis of compounds **5** (●; $\beta_{lg} = -1.102 \pm 0.015$; intercept $= 10.30 \pm 0.12$). The solid line was fitted by linear least-squares regression.

and Katz interpreted their data as supporting a nucleophilic mechanism for the AP-catalyzed reaction.

To suggest that the mechanism of the AP-catalyzed reaction is dissociative[7] solely on the basis of the value of the β_{lg} is misleading. Our data for the hydrolysis **5** support the nucleophilic mechanism (Scheme 1), yet the value of β_{lg} is large (-1.10 ± 0.02, $r = 0.9998$, Figure 6).[26] This parameter first has to be normalized[27] before it is used to estimate the degree of bond cleavage at the transition state and choose between the two mechanisms. In these complexes (**5**), we estimate that the phosphate monoester coordinated to the Co(III) centers resembles an uncoordinated monoester monoanion; that is, the two Co(III) centers have approximately the same effect as a single proton.[28] For equilibrium phenol transfer in monoanionic phosphate esters, $\beta_{eq} = 1.74$, indicating that the aryl oxygen has a partial charge of +0.74 in the starting material (Scheme 3a). Thus, the degree of bond breaking to the leaving group in the transition state is $1.10[0.74 - (-1.0)] = 0.67$. This analysis shows that bond breaking to the leaving group is nowhere near complete in the transition state for hydrolysis of these complexes, with an effective charge of −0.36 on the leaving oxygen in the transition state. Applying a similar analysis to the solution reaction of monoester dianions (Scheme 3b), the degree of bond breaking here is $1.23/1.35 = 0.91$, and the effective charge on the leaving group is −0.88, which is consistent with a dissociative mechanism.[7] Hence, the large value of β_{lg} for the hydrolysis of **5** (and for the AP-catalyzed reaction) does not necessarily indicate a dissociative mechanism. However, once the parameter is properly normalized, it can be used to show that there is only a relatively small fraction of a negative charge on the leaving group oxygen at the transition state (Scheme 3a), in contrast to what is expected for a dissociative mechanism.

Scheme 3. Transition States for Hydrolysis of (a) **5** and (b) Aryl Phosphomonoester Dianions

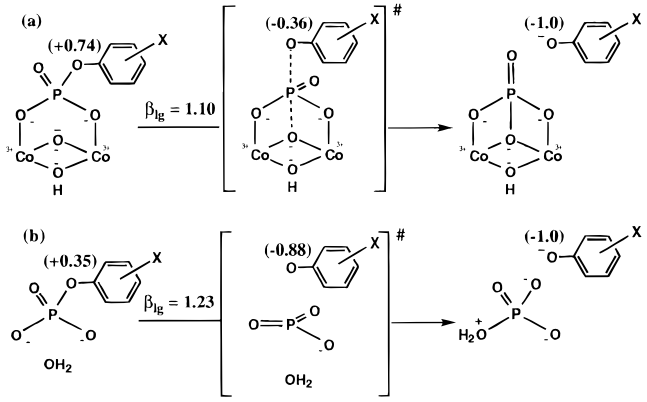

Close to a full negative charge is expected if a dissociative mechanism is involved since, according to the Hammond postulate, the transition state should be late for forming the highly unstable meta-phosphate intermediate (Scheme 3b). In any case, it does not seem reasonable that such a highly reactive intermediate (meta-phosphate) would require the presence of the deprotonated hydroxide (Scheme 1) to be attacked.

Unfortunately, systematically varying the nucleophile to measure the β_{nuc} is clearly not possible for the hydrolysis of **5**. However, an estimate can be made from the two possible nucleophiles that are present: bridging hydroxide and oxide. We estimate that the pK_a of the conjugate acid of the bridging hydroxide is about −1,[29] which compares with a pK_a of 15 for dissociation of the bridging hydroxide (to give the bridging oxide). The first-order rate constant for attack at phosphorus in **5a** is estimated as 3.5×10^4 s^{-1} for oxide and less than 1.0×10^{-6} s^{-1} for hydroxide (no observable deviation from linearity at pH 5.5, where $k_{obs} = 1.0 \times 10^{-5}$ s^{-1} for **5a**). Thus, there are at least a 10.5 orders of magnitude difference in reactivity between the bridging hydroxide and oxide nucleophiles, which can be compared with a difference in pK_a of 16 units, to give an approximate β_{nuc} of ≥0.66. Usually, $\beta_{nuc} \leq 0.3$ for attack of nucleophiles at phosphate monoester dianions;[30] applying this to our values for oxide attack, then the rate of attack of hydroxide should be about 0.5 s^{-1} ($10^{(16 \times -0.3)} \times 3.5 \times 10^4$ s^{-1}), and this would be the only reaction observed for **5a**. Clearly, this estimate disagrees by many orders of magnitude, although **5a** has the best leaving group and is the most likely of these substrates to react by a dissociative mechanism.

In the above discussion, we used the reaction of **5** to demonstrate that the large value of β_{lg} for the AP-catalyzed reaction does not necessarily imply a dissociative mechanism.[7] However, it should be noted that the mechanism for AP-catalyzed hydrolysis of phosphate monoesters[31] is different from the one proposed for the hydrolysis of **5**. The two systems are similar in that they involve dinuclear metal centers for hydrolyzing phosphate monoesters and in that the β_{lg} values for both systems are large. Unlike PP-2B, AP catalyzes transesterification

(26) It should be noted that high values of β_{lg} do not preclude nucleophilic mechanisms. Kirby et al. have shown that large values of β_{lg} are observed for nucleophilic mechanisms of phosphate hydrolysis; for example, for the hydrolysis of diesters catalyzed by nucleophilic attack of an intramolecular carboxylate, $\beta_{lg} = -1.26$ (Khan, S. A.; Kirby, A. J.; Wakselman, M.; Horning, D. P.; Lawlor, J. M. *J. Chem. Soc. (B)* **1970**, 1182), and the attack of triesters by water has $\beta_{lg} = -1.0$ (Khan, S. A.; Kirby, A. J. *J. Chem. Soc. (B)* **1967**, 1172).

(27) Williams, A. *Acc. Chem. Res.* **1984**, *17*, 425. Williams, A. *Chem. Soc. Rev.* **1986**, *15*, 125.

(28) (a) Edwards, J. D.; Foong, S.-W.; Sykes, A. G. *J. Chem. Soc., Dalton Trans.* **1973**, 829. (b) Scott, K. L.; Green, M.; Sykes, A. G. *J. Chem. Soc. (A)* **1971**, 3651.

(29) The pK_a of the bridging hydroxides in triply hydroxide-bridged dinuclear Co(III) complexes has been previously reported as lying in the range 0−1.5 (ref 10); however, these figures, based on kinetic analysis, are likely to be in error (Jentsch, W.; Schmidt, W.; Sykes, A. G.; Wieghardt, K. *Inorg. Chem.* **1977**, *16*, 1935), and so we make this estimate on the basis of the observation that two Co(III) ions have an effect on oxygen similar to that of a single protonation (ref 25). A higher estimate would increase our lower limit for β_{nuc}.

(30) (a) Kirby, A. J.; Jencks, W. P. *J. Am. Chem. Soc.* **1965**, *87*, 3209. (b) Kirby, A. J.; Varvoglis, A. G. *J. Chem. Soc. (B)* **1968**, 168. (c) Herschlag, D.; Jencks, W. P. *Biochemistry* **1990**, *29*, 5172.

(31) Kim, E. E.; Wyckoff, H. W. *J. Mol. Biol.* **1991**, *218*, 449.

of phosphate monoesters, which is incompatible with the oxide mechanism (Scheme 1). Interestingly, a high sensitivity to the leaving group pK_a for the hydrolysis of **5** (Figure 6) provides a strong reason for the presence of potential general acid catalysts in the active site of PP-1. Adding this mode of catalysis to the dinuclear active site would be particularly complementary, providing an enormous additional rate enhancement by effectively activating the leaving group.

Several conclusions can be made regarding the dinuclear Co(III) complexes with bridging phosphate monoesters (**5a**−**d**). First, the crystal structure of **5b** (Figure 5) is closely related to the active site structures of KBPAP (**2**), PP-1 (**3**), and PP-2B (**4**). All of these structures consist of two octahedral metal complexes connected by two oxygen bridges, forming the four-membered-ring diamond core. Additionally, all of the dinuclear centers can be bridged by a phosphate or its analogue. Second, the pH−rate profile (Figure 1) and the ^{18}O labeling experiment (Figure 2) for the hydrolysis of **5b** indicate that the oxide bridging the two metal centers in the diamond core is acting as the nucleophile for cleaving the bridging, double Lewis acid-activated phosphate monoester (Scheme 1). This nucleophilic mechanism not only is viable but also provides greater rate acceleration (Figures 3 and 4) for hydrolyzing the monoester when compared to other mechanisms in other dinuclear model systems (**7**, **8**, and **9**). Third, the oxide mechanism (Scheme 2b) can be used to rationalize the observation that PP-2B does not catalyze transesterification of phosphate monoesters. In principle, the metal hydroxide mechanism (Scheme 2a) should also allow transesterification of phosphate monoesters by the metal alkoxide intermediate. Combining the above data, **5a**−**d** appear to be excellent structural and functional models of the three dinuclear metallophosphatases (KBPAP, PP-1, PP-2B). Finally, the rate of hydrolysis of **5** is highly sensitive to the basicity of the leaving group (Figure 6, $\beta_{lg} = -1.10$), as in the AP-catalyzed hydrolysis of thiophosphate monoesters ($\beta_{lg} = -0.80$). The high sensitivity by itself does not indicate that the hydrolysis reaction in the enzymic or the model system is proceeding by a dissociative mechanism.[7] Proper analysis of the leaving group dependence for the hydrolysis of **5** indicates only a partial negative charge on the leaving group oxygen at the transition state, further supporting the nucleophilic mechanism (Scheme 3a).

Acknowledgment. We thank NSERC, Pioneer Hi-Bred, and the U.S. Army research office for support of this work. The authors are thankful to Dr. Celine Pearson for helpful suggestions regarding the X-ray crystallographic data.

JA9827797